

Magnetic and Thermal Studies of Di-*p*-Anisylnitrosyl\*

WILLIAM DUFFY, JR.

*Department of Physics, University of Santa Clara, Santa Clara, California 95053*

AND

DONALD L. STRANDBURG

*Department of Physics, San Jose State College, San Jose, California 95114*

AND

JOSEPH F. DECK

*Department of Chemistry, University of Santa Clara, Santa Clara, California 95053*

(Received 17 January 1969)

The static magnetic susceptibility from 1.4 to 300°K and the zero-field specific heat from 1.0 to 15°K of the stable aromatic free-radical di-*p*-anisylnitrosyl have been measured on powder samples. The data are shown to be consistent with nearest-neighbor antiferromagnetic Heisenberg exchange ( $S = \frac{1}{2}$ ) of a quadratic layer lattice. The nearest-neighbor exchange integral is estimated to be 2.4°K. Both a discontinuity in  $d\chi/dT$  and a slight indication of an anomaly in the specific heat at 2.7°K indicate a possible antiferromagnetic transition at that temperature. The susceptibility exhibits a Curie-Weiss law  $\chi^{-1} = 2.86(T + 3.4^\circ\text{K})$  mole/emu at high temperatures and a broad maximum at about 4.1°K. The specific heat is resolved into a lattice  $T^3$  contribution characterized by a Debye temperature of  $83.5 \pm 2^\circ\text{K}$ , and a magnetic contribution characterized by an entropy per mole of 98% of the expected  $R \ln 2$ . The magnetic specific heat exhibits a broad maximum at a temperature of about 3.1°K.

## INTRODUCTION

AROMATIC free-radical solids are semiconducting<sup>1</sup> paramagnets at room temperature, often characterized by a small ( $\sim 1$ – $10^\circ\text{K}$ ) antiferromagnetic Weiss constant.<sup>2,3</sup> Because of the lack of symmetry of the stable free radicals, they condense into a crystalline solid which also exhibits low symmetry, and thus the coordination number  $z$  of the unpaired electrons is small.<sup>4</sup> Typically,  $z = 1$  as in *N*-picryl-9-aminocarbazyl or 2,2-bis(*p*-nitrophenyl)-1-picrylhydrazyl, or  $z = 2$  as suggested for 2-phenyl-2-*p*-nitrophenyl-1-picrylhydrazyl.<sup>5</sup> The radical solid di-*p*-anisylnitrosyl [DPAN,  $(\text{H}_3\text{COC}_6\text{H}_4)_2\dot{\text{N}}\text{O}$ , more commonly called di-*p*-anisyl nitric oxide] exhibits  $z = 4$  and is a magnetically layered crystal, as inferred from the x-ray crystallographic study of Hanson.<sup>6</sup>

The radical DPAN is orthorhombic at room temperature<sup>6</sup> with four molecules per unit cell ( $a = 7.33 \pm 0.04$ ,  $b = 26.8 \pm 0.1$ ,  $c = 6.25 \pm 0.03$  Å). The space group is *Aba*2. Two orthogonal projections of the unit cell are seen in Fig. 1. The (010) projection, which exhibits the planar network of nitrogen radicals is shown in Fig. 1(b). The nitrogen radicals form parallel rhombic plane nets normal to the  $b$  axis. Within the planes the nearest-neighbor distance is 4.81 Å, the next-nearest-neighbor distance is 6.25 Å and the next-next-nearest-neighbor distance is 7.33 Å. In adjacent planes the nearest-

neighbor nitrogen radicals are separated by  $\frac{1}{2}(\pm \mathbf{b} \pm \mathbf{a} \pm \mathbf{c})$ , corresponding to a nearest-interplane-neighbor distance of 13.8 Å. It may thus be inferred that interplane exchange should be very small compared to intraplane exchange, and to a first approximation, considering only nearest-neighbor exchange, the magnetic lattice may be considered a planar quadratic net. The magnetic and thermal measurements reported here tend to support this conjecture.

Although many layered magnetic crystals have been studied,<sup>7</sup> few are characterized by an interlayer exchange which is much smaller than the intralayer exchange so that one may neglect the interaction of neighboring layers with a given layer in analyzing the magnetic structure. Indeed, the system  $\text{K}_2\text{NiF}_4$  and its isomorphs, as pointed out by Lines,<sup>8,9</sup> are the only clearly established examples of antiferromagnetic structures ordered on an intraplane, but not on an interplane basis.

In the next two sections, a description is presented of static susceptibility measurements of DPAN from 1.4 to 300°K and specific-heat measurements of DPAN from 1.0 to 15°K. In the last section of this paper, the results are analyzed using the theories of the quadratic layer Heisenberg net.

## EXPERIMENTAL DETAILS

The DPAN samples were freshly prepared for the measurements described herein according to the pro-

\* Supported by the National Science Foundation.

<sup>1</sup> D. D. Eley, K. W. Jones, and M. R. Willis, *Nature* **212**, 72 (1966).<sup>2</sup> W. Duffy, Jr., *J. Chem. Phys.* **36**, 490 (1962).<sup>3</sup> W. Duffy, Jr. and D. Strandburg, *J. Chem. Phys.* **46**, 456 (1967).<sup>4</sup> H. M. McConnell and R. Lynden-Bell, *J. Chem. Phys.* **36**, 2393 (1962).<sup>5</sup> W. Duffy, Jr. and K. P. Barr, *Phys. Rev.* **165**, 647 (1968).<sup>6</sup> A. W. Hanson, *Acta Cryst.* **6**, 32 (1953).<sup>7</sup> A. R. Miedema, *Proceedings of International Institute of Refrigeration*, 1967 (unpublished); C. Domb and A. R. Miedema, in *Progress in Low Temperature Physics*, edited by C. J. Gorter (North-Holland Publishing Co., Amsterdam, 1964), Vol. IV, p. 325; J. S. Smart, in *Magnetism*, edited by G. T. Rado and H. Suhl (Academic Press Inc., New York, 1963), Vol. III, p. 101.<sup>8</sup> M. E. Lines, *Phys. Letters* **24A**, 591 (1967).<sup>9</sup> M. E. Lines, *Phys. Rev.* **164**, 736 (1967).

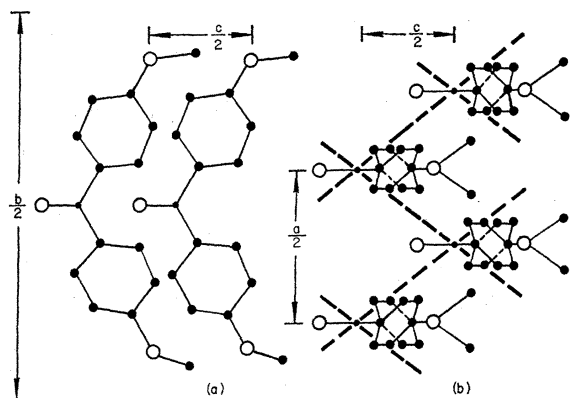


FIG. 1. (a) Two of the four DPAN molecules in the unit cell as viewed on a (100) projection. In this projection, the other two molecules in the unit cell appear identical to these two, but are displaced by  $\frac{1}{2}b$ . (b) Four neighboring molecules of DPAN as viewed on a (010) projection. The dashed lines indicate shortest paths between nearest-neighbor N radicals. O:  $\circ$ , N:  $\bullet$ , C:  $\bullet$ .

cedure of Meyer and Gottlieb-Bielroth.<sup>10</sup> The copper-colored crystals were typically thin platelets of area  $10^{-3}$  cm<sup>2</sup>. The susceptibility sample analyzed C:68.37, H:5.72, and exhibited a 148–150°C mp. The specific-heat sample analyzed C:68.53, H:5.97, and exhibited a 150°C mp. The calculated analysis for C<sub>14</sub>H<sub>14</sub>NO<sub>3</sub> is C:68.84, H:5.78. The observed sintering temperature of 120°C and mp of 150°C were in accord with the published values.<sup>10</sup>

The susceptibility measurements were done in a Faraday balance apparatus using an electrobalance similar to the one described by McGuire and Lane.<sup>11</sup> The sample is suspended from a quartz fibre in an inhomogeneous magnetic field of 5 kG or less and surrounded by a pressure of about 1000 Torr of <sup>4</sup>He ex-

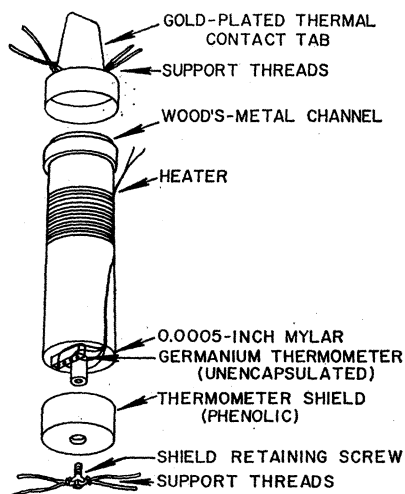


FIG. 2. Calorimeter sample can. The can and can cover are machined from OFHC Cu. The powdered sample and 0.1 atm of <sup>4</sup>He exchange gas are sealed into the container.

<sup>10</sup> K. H. Meyer and H. Gottlieb-Bielroth, Chem. Ber. **52B**, 1476 (1919); Chem. Abstr. **14**, 1533 (1920).

<sup>11</sup> T. R. McGuire and C. T. Lane, Rev. Sci. Instr. **20**, 489 (1949).

change gas. The cylindrical OFHC copper walls, concentric with the sample and its suspension, are isolated from a LHe or LN<sub>2</sub> bath by a concentric vacuum region. Temperatures above the bath temperature are obtained by electrically heating the copper walls. Lower temperatures are obtained by introducing <sup>4</sup>He gas into the vacuum region and pumping on the bath. In good thermal contact with the concentric Cu tube, a Honeywell Ge resistance thermometer and a Cu resistance thermometer are used to determine sample temperature in the 1–40°K and 40–300°K temperature ranges, respectively. For the Ge thermometer, a manufacturer's calibration gives the temperature to  $\pm 0.1^\circ\text{K}$  for the range 4.2–40°K. The Ge thermometer was immersed in the <sup>4</sup>He bath for calibration against the helium vapor pressure from 1.4 to 4.2°K with an estimated accuracy of  $\pm 0.01^\circ\text{K}$ . The Cu thermometer was calibrated at the normal bp of N and the ice point of water, using the universal curve of Dauphinee and Preston-Thomas<sup>12</sup> and Mathiessen's rule, and the temperatures so determined are estimated to be within  $\pm 0.5^\circ\text{K}$ . The electrobalance output is amplified and fed back through a Fairchild ADO-22 operational amplifier to the balance coil. The coil current is read by a Non-Linear Systems 5010 digital meter. Absolute susceptibilities are determined using a 99.999% pure Pt cylinder, obtained from Alpha Scientific, assuming the room-temperature Pt susceptibility to be  $0.968 \times 10^{-6}$  emu/g. The relative susceptibilities are reliable to about  $\pm 0.5\%$  of the He temperature values. Absolute calibration is correct to within about  $\pm 5\%$ .

The specific-heat cryostat is an intermittent-heating <sup>4</sup>He-cooled apparatus of conventional design, somewhat similar to one described by Scurlock and Wray.<sup>13</sup> By using a 4.2°K shield bath surrounding the pumped inner <sup>4</sup>He bath, temperatures as low as 0.98°K are obtained using a Welch 1397 13-ft<sup>3</sup>/min pump.

The details of the OFHC copper sample container are shown in Fig. 2. A mechanical heat switch provides thermal contact from the <sup>4</sup>He bath to the tab on the sample can top, and no heat-exchange gas is used. The container cap is soldered to the container with Wood's metal in about 0.1 atmosphere of He gas. A manganin heater is wound on the cylindrical surface and the bare Ge resistance thermometer is cemented with GE 7031 adhesive to a 0.0005-in. insulating Mylar sheet, which is in turn cemented to the bottom of the container. The thermometer is calibrated against the <sup>4</sup>He vapor pressure below 4.2°K and against a Honeywell Ge thermometer calibrated by the manufacturer above 4.2°K. The discrete calibration points are used to generate a continuous resistance-temperature curve by least-squares fitting on a computer to a curve of the form

$$\ln R = \sum_{n=0}^{10} C_n (\ln T)^n,$$

<sup>12</sup> T. M. Dauphinee and H. Preston-Thomas, Rev. Sci. Instr. **25**, 884 (1954).

<sup>13</sup> R. G. Scurlock and E. M. Wray, J. Sci. Instr. **42**, 421 (1965).

as used by Osborne,<sup>14</sup> where  $R$  is the resistance,  $T$  is the absolute temperature, and the  $C_n$  are eleven coefficients determined by the least-squares criteria. A three-wire connection is made to the thermometer which forms one arm of a Wheatstone bridge operated at 33 Hz, similar to one described by Blake, Chase, and Maxwell.<sup>15</sup> The power level in the thermometer is  $10^{-9}$  W or less below 4°K. The heater current is supplied through a standard resistor, the terminal voltage of which is measured by a Non-Linear Systems 5010 digital voltmeter. The heater resistance is measured by the usual four-terminal technique with a Leeds and Northrup type K-2 potentiometer. The heating intervals are determined by a Berkeley Type 5120BC time-interval meter. Corrections are made for the heat leak during the heat-on period by extrapolating the thermometer resistance *versus* time curve immediately before and after the heat pulse to a point at the middle of the heat pulse. The bridge off-balance resistance versus time (after amplification and phase-sensitive detection) is recorded on a Bausch and Lomb VOM6 strip chart recorder.

### MEASUREMENTS

Susceptibility measurements were performed on two independently prepared samples of DPAN. The two sets of results were in substantial agreement. The results for the chemically purer sample are reported here and shown in Figs. 3 and 4. Some difficulty was experienced initially in obtaining the susceptibility data, since below about 150°K the fused-quartz sample bucket was pulled into the wall of its cylindrical copper enclosure. This was attributed to a buildup of static charges on the sample because of its pyroelectricity, which charges would then be attracted to images in the conducting wall. The pyroelectricity is consistent with the space group *Aba2*. Why this effect set in below about 150°K is not known. Perhaps there is a crystalline transition in that vicinity which enhances the pyroelectricity below the transition temperature or a ferroelectric transition may occur. This difficulty was overcome by replacing the quartz bucket with a much heavier Teflon bucket, setting up a sufficient restoring torque to prevent the electric torque from pulling the sample into the enclosure wall. The susceptibility of the Teflon bucket was determined in a separate measurement and subtracted from the measured (sample + bucket) susceptibilities.

The raw data were corrected for the bucket diamagnetism and converted to absolute data by comparison with measurements on the Pt standard. The paramagnetic susceptibility was then obtained by subtracting off the calculated diamagnetic contribution of  $-138 \times 10^{-6}$  emu/mole.<sup>16</sup> The paramagnetic susceptibility  $\chi$  follows a Curie-Weiss law for temperatures

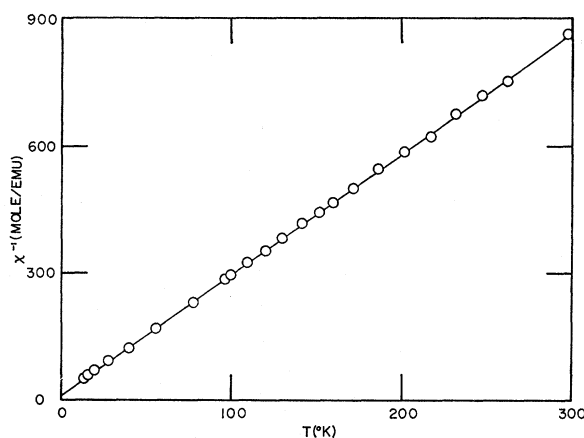


FIG. 3. Inverse paramagnetic susceptibility of DPAN versus temperature. The straight line shown corresponds to  $\chi^{-1} = 2.86(T+3.4)$  mole/emu. It is a least-squares fit to the data shown from 77 to 300°K.

$T \gtrsim 30^\circ\text{K}$ , as shown in Fig. 3. The straight-line plot corresponding to  $\chi^{-1} = 2.86(T+3.4)$  mole/emu was determined by least squares for the experimental points shown with  $T > 77^\circ\text{K}$ . This agrees rather well with the measurements of Müller *et al.*<sup>17</sup> above 90°K, which gave  $\chi^{-1} = 2.74(T+3)$  mole/emu. At about 4.1°K the  $\chi$  *versus*  $T$  curve (Fig. 4) exhibits a rather flat maximum of  $28.7 \times 10^{-3}$  emu/mole and drops off to an extrapolated absolute-zero susceptibility of  $20.0 \times 10^{-3}$  emu/mole. There is an indication of a discontinuity in  $d\chi/dT$  at about 2.7°K, which was also seen in the measurement on the less-pure sample.

Results of the heat-capacity measurements are shown in Figs. 5-7. The data were taken on a 0.525 g powder sample and have been corrected for the specific heat of the addenda, as determined in a separate measurement. This correction amounted to 2% at 1°K, 3% at 2°K, 11% at 4°K, 47% at 8°K, and 53% at 12°K. The lattice

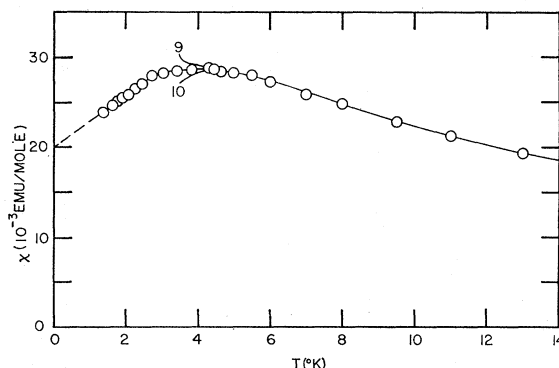


FIG. 4. Low-temperature paramagnetic susceptibility of DPAN versus temperature. The curves marked 9 and 10 correspond to the high-temperature expansion of Eq. (3) for 9 and 10 terms, respectively. The fit of the theoretical curve has been effected by choosing  $|J|/k = 2.35^\circ\text{K}$  and multiplying the theoretical curve by a constant factor of  $p = 0.95$ .

<sup>14</sup> Darrell W. Osborne, *Ann. Acad. Sci. Fennicae: Ser. A*, VI, 210, 53 (1966).

<sup>15</sup> C. Blake, C. E. Chase, and E. Maxwell, *Rev. Sci. Instr.* 29, 715 (1958).

<sup>16</sup> A. Pacault, *Rev. Sci.* 86, 38 (1948).

<sup>17</sup> E. Müller, I. Müller-Rodloff, and W. Bunge, *Ann. Chem.* 520, 235 (1935).

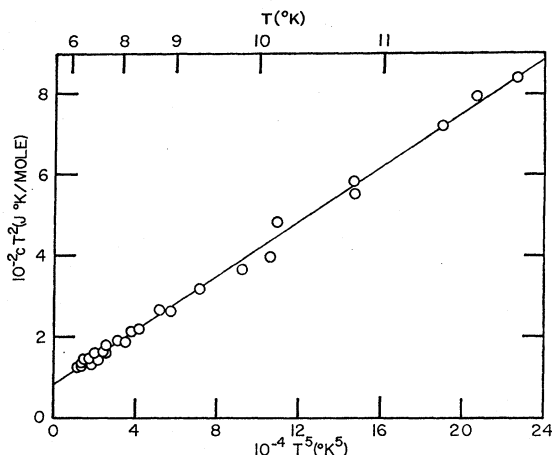


FIG. 5. Least-squares straight-line plot of  $cT^2$  versus  $T^5$  from 6 to 12°K. The straight line shown corresponds to  $cT^2 = (0.00334T^5 + 85) \text{ J } ^\circ\text{K/mole}$ .

contribution is separated from the specific heat of the exchange system by assuming an expression of the form

$$c/R = 234(T/\Theta_D)^3 + (\Lambda/T)^2, \quad (1)$$

where  $c$  is the total molar heat capacity,  $R$  is the gas constant per mole,  $\Theta_D$  is the lattice Debye temperature, and  $\Lambda$  is a constant characteristic of the exchange interactions. A least-squares fit of the data from 6.5 to 12°K to this expression is shown in Fig. 5. The Debye temperature  $\Theta_D$  is found to be  $(83.5 \pm 2)^\circ\text{K}$  and  $\Lambda$  is  $(3.19 \pm 0.19)^\circ\text{K}$ . The resultant magnetic specific-heat curve is obtained by subtracting the  $T^3$  term given by (1) from the total  $c$ , and this is plotted in Fig. 6.

TABLE I. Specific heat of di-*p*-anisyl nitrosyl from 1 to 15°K. The values given correspond to data averaged over intervals of 0.1° (0.9–4.5°K), 0.25° (4.5–6°K), 0.5° (6–9°K), and 1.0° (9–15°K).

$T$ (°K)	$c$ (J/mole °K)	$T$ (°K)	$c$ (J/mole °K)
0.982	0.465	3.543	3.48
1.046	0.610	3.662	3.38
1.145	0.790	3.758	3.32
1.213	0.925	3.850	3.24
1.310	1.094	3.950	3.27
1.435	1.403	4.031	3.19
1.553	1.691	4.13	3.13
1.631	1.883	4.26	3.21
1.726	2.077	4.34	3.15
1.818	2.325	4.46	3.13
1.923	2.568	4.69	3.01
2.042	2.759	5.03	3.06
2.143	2.98	5.39	2.84
2.239	3.10	5.81	2.86
2.349	3.18	6.29	3.05
2.454	3.25	6.74	3.03
2.547	3.34	7.20	2.84
2.649	3.35	7.68	3.03
2.749	3.47	8.24	3.08
2.846	3.48	8.75	3.40
2.942	3.47	9.46	3.86
3.046	3.51	10.51	4.58
3.150	3.53	11.6	5.87
3.244	3.53	12.5	6.50
3.355	3.43	13.4	7.59
3.445	3.48	14.1	8.20

The contribution to the magnetic entropy below 1°K is determined from the smooth extrapolation indicated on Fig. 6. For  $1^\circ\text{K} < T < 7.4^\circ\text{K}$ , the magnetic entropy is determined from the smooth curve through the data plotted in Fig. 6. For  $T > 7.4^\circ\text{K}$ , the magnetic entropy contribution is simply  $s_M(\infty) - s_M(7.4) = \frac{1}{2}R(\Lambda/7.4)^2$ . The total magnetic entropy  $s_M(\infty) - s_M(0)$  is found to be 0.984 of the expected  $R \ln 2$ . This rather good agreement with the expected entropy is of interest because of a suggestion<sup>18</sup> that for organic radicals the correct magnetic entropy might differ from  $R \ln 2$ .

The energy corresponding to the integral of the magnetic specific heat over all temperatures is determined below 7.4°K from the smooth curve plotted in Fig. 6. The contribution to the energy above 7.4°K is simply  $R\Lambda^2/7.4$ .

The total specific heat per mole of DPAN from 1 to 15°K is given by the averaged data shown in Fig. 7. These data are also given in Table I.

## INTERPRETATION AND DISCUSSION

In organic free radicals, electron spin resonance results indicate a  $g$  value very close to the free-electron value. This implies small spin-orbit interaction and, as a consequence, isotropic exchange.<sup>19</sup> In DPAN  $g_{11} = 2.0095$  and  $g_{12} = 2.0043$ <sup>20</sup> compared to the free-electron value of 2.0023. A Heisenberg exchange Hamiltonian ( $S = \frac{1}{2}$ ) is thus appropriate to describe the magnetic system, and it may be written in the form

$$\mathcal{H} = +2|J| \sum \mathbf{S}_i \cdot \mathbf{S}_j, \quad (2)$$

where the sum is over all nearest-neighboring spins  $\mathbf{S}_i$  and  $\mathbf{S}_j$  and  $J$  is the exchange integral, assumed equal for all nearest-neighboring spin pairs.

Dipolar interactions have been neglected in writing (2). Using the lattice parameters determined by Hanson<sup>6</sup> and assuming magnetization normal to the plane of the net, an estimate of the local dipole field is calculated by a direct sum over all dipoles in a rectangular parallelepiped of dimensions  $20a \times 10b \times 20c$ . This yields a dipolar field of  $H_d \approx -4.08 \times 10^{22} (M/N)$ , where  $M$  is the magnetization and  $N$  is the number of spins. This may be compared to the "exchange field" of  $H_e = z|J|M/(Ng^2\beta^2)$ , where  $g$  is the  $g$  factor and  $\beta$  is the Bohr magneton. For  $|J|/k = 2.4^\circ\text{K}$ , these expressions give  $|H_d/H_e| \approx 0.011$ , justifying the neglect of the anisotropic dipolar interactions for discussing the paramagnetic phase of DPAN. At very low temperatures, the "small" anisotropy is no longer ignorable. It leads to a finite energy gap at zero wave vector in the spin-wave spectrum, which profoundly affects the thermodynamic properties, at least for  $kT$  of the order of this gap energy, where  $k$  is Boltzmann's constant.

<sup>18</sup> W. O. Hamilton and G. E. Pake, *J. Chem. Phys.* **39**, 2694 (1963).

<sup>19</sup> William Low, in *Solid State Physics*, edited by F. Seitz and D. Turnbull (Academic Press Inc., New York, 1960), Suppl. 2, p. 155.

<sup>20</sup> A. van Roggen, L. van Roggen, and W. Gordy, *Phys. Rev.* **105**, 50 (1957).

The eigenspectrum of Eq. (2) for the quadratic net is not known. For  $T > |J|/k$ , exact high-temperature expansions of the partition function using trace evaluations have yielded series in powers of  $|J|/kT$  for the susceptibility and specific heat. The ten-term series which was used to calculate the susceptibility of a spin- $\frac{1}{2}$  Heisenberg quadratic net is

$$4\chi|J|/Ng^2\beta^2 = \alpha - 2\alpha^2 + 2\alpha^3 - 4\alpha^4/3 + 13\alpha^5/12 - 71\alpha^6/60 \\ + 367\alpha^7/720 + 811\alpha^8/2520 \\ + 8213\alpha^9/20160 - 1729\alpha^{10}/1620, \quad (3)$$

where  $\alpha = |J|/kT$ . The coefficients in Eq. (3) were calculated from the results of Rushbrooke and Wood<sup>21</sup> and Domb and Wood,<sup>22</sup> with reference to the tables of Domb.<sup>23</sup> The fitted curves corresponding to 9 and 10 terms of Eq. (3) are indicated in Fig. 4. The fitting parameters are  $|J|/k = 2.35 \pm 0.05^\circ\text{K}$  and an amplitude parameter  $p = 0.95$ , which may be compared with the corresponding values obtained from the least-squares Curie-Weiss law in the high-temperature region of  $p = 0.93$  and  $\frac{1}{2}\Theta = -|J|/k = -(1.7 \pm 0.5)^\circ\text{K}$ . The value of the Weiss constant  $\Theta$  is obtained from data in the 77–300°K region, whereas the determination of  $|J|$  from the fit of Eq. (3) to the experimental susceptibility depends mainly on the low temperature ( $\sim 4$ –40°K) data. Thus, the smaller  $|J|$  determined from the Weiss constant *may* indicate a temperature-dependent exchange integral resulting from thermal expansion of the lattice. The Weiss constant is unfortunately very uncertain, since it is sensitive to the accuracy of both the diamagnetic correction and the calibration. The  $\pm 0.5^\circ\text{K}$  quoted here results from scatter in the data and the 5% uncertainty in the calibration. There is an additional unknown systematic uncertainty because of uncertainty of the diamagnetic correction.

The specific-heat series converges rather slowly, so that the limiting curve in the vicinity of the specific-heat maximum is very uncertain and a fitting to the data such as was effected with the susceptibility curve is not feasible. The coefficient of the leading  $T^{-2}$  term in the expansion may be compared with the measured coefficient to obtain another measure of  $|J|$ . This gives  $|J|/k = (\sqrt{\frac{2}{3}})\Delta = (2.60 \pm 0.15)^\circ\text{K}$ .

For a Hamiltonian with a zero trace, the ground-state energy is equal to the negative of the integral of the corresponding specific heat, integrated over all temperatures. Equation (2) is an example of such a Hamiltonian. Thus we infer the ground-state energy  $E_0$  of DPAN to be  $-(27.5 \pm 1.4)$  J/mole. Anderson<sup>24</sup> has shown that the ground-state energy (per mole) corresponding to (2) is bounded according to the inequality

$$-R(|J|/k)zS^2 > E_0 > -R(|J|/k)zS^2(1 + 1/Sz), \quad (4)$$

where  $S$  is the spin. The only restriction on this in-

<sup>21</sup> G. S. Rushbrooke and P. J. Wood, *Mol. Phys.* **1**, 257 (1958).

<sup>22</sup> C. Domb and P. J. Wood, *Proc. Roy. Soc. (London)* **86**, 1 (1965).

<sup>23</sup> C. Domb, *Advan. Phys.* **9**, 329 (1960).

<sup>24</sup> P. W. Anderson, *Phys. Rev.* **83**, 1260 (1951).

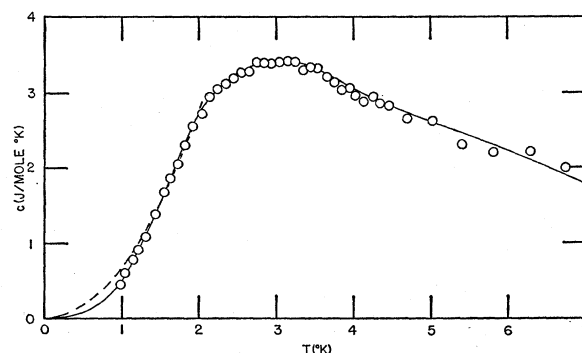


FIG. 6. Magnetic specific heat of DPAN versus temperature. The smooth curve shown was used to calculate the energy and entropy. The dashed line corresponds to  $c = (0.691T^2)$  J/mole.

equality is that the magnetic lattice must be divisible into two sublattices so that each spin on a given sublattice has all nearest neighbors on the other sublattice. This is obviously satisfied for the quadratic net. Using our experimental result for  $E_0$ , we obtain from (4) the result  $2.20^\circ\text{K} < |J|/k < 3.30^\circ\text{K}$ .

Low-temperature approximate approaches to the Heisenberg antiferromagnet include the spin-wave theories of Anderson,<sup>25</sup> Kubo<sup>26</sup> and others and the double-time temperature-dependent Green-function method.<sup>27</sup> The spin-wave theory of Kubo, which takes account of spin-wave interactions to first order, gives for the ground-state energy (per mole) of the quadratic plane net, to order  $1/S$ , the result

$$E_0/R = -zS(S + 0.158 + 0.0062S^{-1})|J|/k. \quad (5)$$

Note that this satisfies Anderson's criterion, Eq. (4). For spin  $\frac{1}{2}$  and  $E_0/R = -3.30^\circ\text{K}$ , Eq. (5) gives  $|J|/k = (2.46 \pm 0.13)^\circ\text{K}$ .

Spin-wave theory predicts a specific heat proportional to  $T^2$  for a two-dimensional lattice at sufficiently low temperatures. The expression for the quadratic net, as given by Kubo,<sup>26</sup> is  $c/R = 0.945(kT/JS)^2$ . The DPAN

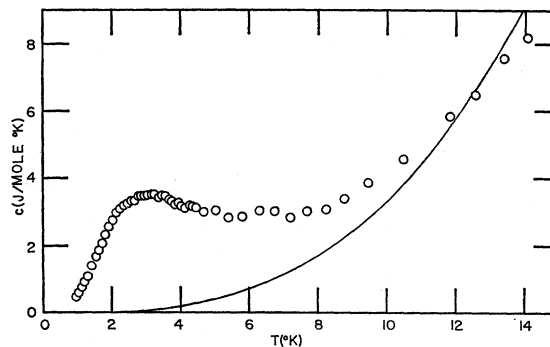


FIG. 7. Specific heat of DPAN versus temperature. The points shown are also given in Table I. The curve is the calculated lattice  $T^3$  term determined in the region from 6 to 12°K by fitting the data to Eq. (1).

<sup>25</sup> P. W. Anderson, *Phys. Rev.* **86**, 694 (1952).

<sup>26</sup> R. Kubo, *Phys. Rev.* **87**, 568 (1952).

<sup>27</sup> M. E. Lines, *Phys. Rev.* **135**, A1336 (1964).

TABLE II. Exchange constant  $|J|/k$  of di-*p*-anisyl nitrosyl as determined from various experimental data assuming quadratic Heisenberg nets. Only experimental error limits are given.

Experimental origin	Theory	$ J /k$ ( $^{\circ}\text{K}$ )
Susceptibility 77–300 $^{\circ}\text{K}$	exact	$1.7 \pm 0.5$
Specific heat 6–12 $^{\circ}\text{K}$	exact	$2.60 \pm 0.15$
Susceptibility 3–300 $^{\circ}\text{K}$	exact	$2.35 \pm 0.05$
$T^2$ magnetic specific heat, 1.2–1.8 $^{\circ}\text{K}$	spin-wave	$2.14 \pm 0.05$
Extrapolated susceptibility 0 $^{\circ}\text{K}$	spin-wave	$1.40 \pm (?)$
Integrated magnetic specific heat	mean value from Anderson <sup>a</sup> limits	$2.64 \pm 0.13$
Integrated magnetic specific heat	spin-wave	$2.46 \pm 0.13$

<sup>a</sup> Reference 24.

specific-heat data are found to follow a  $T^2$  dependence in the 1.4–1.9 $^{\circ}\text{K}$  temperature range, as shown in Fig. 6. The coefficient corresponds to  $|J|/k = (2.14 \pm 0.05)^{\circ}\text{K}$ . Below 1.4 $^{\circ}\text{K}$  the data points are lower than this  $T^2$  curve, which may be attributed to the dipolar anisotropy.

The exchange integral may also be estimated from the zero temperature susceptibility. The spin-wave result<sup>28</sup> is

$$\chi(0) = \frac{2}{3}\chi_1(0) = (0.448)Ng^2\beta^2/(24|J|), \quad (6)$$

where the assumption of randomly oriented crystals gives the factor of  $\frac{2}{3}$ . If the extrapolated  $T=0$  susceptibility seen in Fig. 4 is used in this expression, the result is  $|J|/k = 1.40^{\circ}\text{K}$ . This is substantially lower than the other determinations. It may be partially attributed to the inaccuracy of the extrapolation. The small crystals are mostly very thin platelets which may preferentially stack in the sample bucket so as to require an increase of the  $\frac{2}{3}$  factor in Eq. (6). This would increase  $|J|$  to a value more consistent with the other determinations. Also important is the presence of paramagnetic impurity effects in the solid free radicals,<sup>3</sup> which may add substantially to the measured susceptibility at the lowest temperatures, thus yielding a low value of  $|J|$ . The Green-function theory gives essentially the same result as Eq. (6), with a coefficient of 0.523 instead of 0.448.

The results of the various determinations of  $|J|/k$  are given in Table II. The data are consistent with a Heisenberg quadratic net characterized by  $|J|/k \approx 2.4^{\circ}\text{K}$ .

Notably absent from the specific heat is a clear indication of the sharp peak characteristic of a cooperative transition to an ordered state. The susceptibility measurements reported here were made prior to the specific-heat measurements and, because of the apparent discontinuity in  $d\chi/dT$  near 2.7 $^{\circ}\text{K}$ , special attention was given to the specific-heat data in this vicinity. A large number of data points were collected from different runs. There is a slight indication of an anomaly at 2.7 $^{\circ}\text{K}$  in the specific heat which we believe is not just

experimental scatter, although it is close to the threshold of resolution at that temperature. This may be seen from the data shown in Fig. 6. Theoretically, two-dimensional systems are found to exhibit very-long-range spin correlations above the transition temperature as compared to three-dimensional systems.<sup>9</sup> The specific-heat anomaly at the transition temperature would thus be expected to involve a relatively small entropy change and this may help to explain the lack of a pronounced anomaly at 2.7 $^{\circ}\text{K}$ .

Mermin and Wagner<sup>29</sup> have rigorously demonstrated that a transition to a long-range-ordered state cannot occur at a finite temperature for a two-dimensional Heisenberg system. Stanley and Kaplan,<sup>30</sup> based on extrapolations of high-temperature expansions of the susceptibility, predict a transition. It may well be that a transition does occur at the temperature inferred from the expansions, which is of the usual spontaneous sublattice magnetization type if there is small but nonzero anisotropy or interlayer exchange. Given the complete absence of anisotropic exchange or interlayer exchange, the transition may be to the peculiar zero-magnetization infinite-initial-susceptibility state suggested by Stanley and Kaplan,<sup>30</sup> and not excluded by the result of Mermin and Wagner.

In the quadratic-layer Heisenberg antiferromagnets  $\text{K}_2\text{MnF}_4$  ( $S = \frac{5}{2}$ ),  $\text{Rb}_2\text{MnF}_4$  ( $S = \frac{5}{2}$ ), and  $\text{K}_2\text{NiF}_4$  ( $S = 1$ ), phase transitions have been found,<sup>31</sup> based on single-crystal susceptibility anisotropy and neutron diffraction.<sup>32</sup> The corresponding values of  $kT_N/|J|$ , where  $T_N$  is the transition temperature, are 11.0, 11.7, and 2.31.<sup>31</sup> Thus, the value of  $kT_N/|J| = 2.7/2.4 = 1.12$  for DPAN ( $S = \frac{1}{2}$ ) is not inconsistent with the experimental results of  $kT_N/|J|$  for other quadratic-layer Heisenberg antiferromagnets, considering the spin-dependence of this parameter.

#### ACKNOWLEDGMENTS

The authors wish to thank John Maita of Bell Telephone Laboratories for his helpful suggestions on calorimetry and for his gift of a Si resistance thermometer which was used in our early calorimetric work. We profited greatly from conversations with Professor William Hamilton. We are also happy to acknowledge the substantial contributions of Wayne Angel, Kevin Barr, Robert Bortfeld, Frank Costanzi, Robert Hausman, Richard Nuccitelli, Arthur Snyder, and Kathleen Weland, all of whom were undergraduate participants in this National Science Foundation sponsored research.

<sup>29</sup> N. D. Mermin and H. Wagner, Phys. Rev. Letters **17**, 1133 (1966).

<sup>30</sup> H. E. Stanley and T. A. Kaplan, Phys. Rev. Letters **17**, 913 (1966).

<sup>31</sup> G. de Vries, D. J. Breed, E. P. Maarschall, and A. R. Miedema, J. Appl. Phys. **39**, 1207 (1968); K. G. Srivastava, Phys. Letters **4**, 55 (1963); D. J. Breed, Physica **37**, 35 (1967).

<sup>32</sup> R. Plumier, J. Appl. Phys. **35**, 950 (1964).

<sup>28</sup> T. Oguchi, Phys. Rev. **117**, 117 (1960).